Salmonella Typhimurium uses the Cpx stress response to detect N -chlorotaurine and promote the repair of oxidized proteins

Camille Andrieu, Laurent Loiseau, Alexandra Vergnes, Séverine Gagnot, Romain Barré, Laurent Aussel, Jean-François Collet, Benjamin Ezraty

PNAS RESEARCH ARTICLE | MICROBIOLOGY OPEN ACCESS

Salmonella Typhimurium uses the Cpx stress response to detect *N*-chlorotaurine and promote the repair of oxidized proteins

Camille Andrieu[a], Laurent Loiseau[a], Alexandra Vergnes[a], Séverine Gagnot[a], Romain Barré[b], Laurent Aussel[a], Jean-François Collet[c], and Benjamin Ezraty[a,1]

Edited by Gisela Storz, National Institute of Child Health and Human Development, Bethesda, MD; received September 19, 2022; accepted March 1, 2023

The cell envelope of gram-negative bacteria constitutes the first protective barrier between a cell and its environment. During host infection, the bacterial envelope is subjected to several stresses, including those induced by reactive oxygen species (ROS) and reactive chlorine species (RCS) produced by immune cells. Among RCS, *N*-chlorotaurine (*N*-ChT), which results from the reaction between hypochlorous acid and taurine, is a powerful and less diffusible oxidant. Here, using a genetic approach, we demonstrate that *Salmonella* Typhimurium uses the CpxRA two-component system to detect *N*-ChT oxidative stress. Moreover, we show that periplasmic methionine sulfoxide reductase (MsrP) is part of the Cpx regulon. Our findings demonstrate that MsrP is required to cope with *N*-ChT stress by repairing *N*-ChT-oxidized proteins in the bacterial envelope. By characterizing the molecular signal that induces Cpx when *S.* Typhimurium is exposed to *N*-ChT, we show that *N*-ChT triggers Cpx in an NlpE-dependent manner. Thus, our work establishes a direct link between *N*-ChT oxidative stress and the envelope stress response.

Salmonella Typhimurium | CpxRA | oxidative stress | oxidized protein

Significance

The Cpx-mediated envelope stress response is crucial for envelope maintenance in Gram-negative bacteria. Strikingly, researchers have reported very few natural stresses that induce the Cpx pathway. Here, we report that a potent antimicrobial reactive chlorine species, *N*-chlorotaurine, activates the Cpx pathway in *Salmonella* Typhimurium, leading to overproduction of the periplasmic oxidized-protein repair system, among other effects. This work presents direct evidence indicating that bacteria use the envelope stress response to detect specific oxidative stress.

Salmonella enterica subsp. *enterica* serovar Typhimurium is a facultative intracellular pathogen associated with a range of infections in mammals, spanning from self-limiting gastroenteritis to severe systemic diseases. The establishment of infection depends on the ability of the pathogen to adapt and resist host defense mechanisms. *S.* Typhimurium infection induces a strong inflammatory cellular response, with a high number of recruiting neutrophils in the intestinal tissues of human patients (1).

The antimicrobial activity of neutrophils relies on their ability to phagocytize the invading microorganism and release lethal concentrations of reactive antimicrobial oxidants. Generally termed as an "oxidative burst," the neutrophil antimicrobial response encompasses the release of a wide variety of reactive oxygen species (ROS) and reactive chlorine species (RCS), which are synthesized by enzymatic pathways involving reduced nicotinamide adenine dinucleotide phosphate oxidase (Nox) and myeloperoxidase (MPO), respectively (2). The Nox-catalyzed neutrophil oxidative burst involves the primary reduction of O_2 to the superoxide radical $O_2^{\cdot-}$, which then dismutates into hydrogen peroxide (H_2O_2) and O_2. MPO catalyzes the oxidation of chloride in the presence of H_2O_2 to generate hypochlorous acid (HOCl), a potent antimicrobial oxidant (3). It has been proposed that HOCl production may be a strategy developed by the host to efficiently kill microorganisms while limiting collateral tissue damage (4). Together, ROS and RCS damage the cellular components (i.e., DNA, membrane lipids, and proteins) of invading bacteria, which can lead to cell death. Therefore, bacteria have evolved defense mechanisms, including the expression of scavengers to convert oxidants to innocuous products and the production of repair enzymes to rescue oxidatively damaged proteins (5–7).

In proteins, methionine (Met) residues are particularly vulnerable to oxidation: they form methionine sulfoxides (Met-O), which can alter secondary or tertiary structures and therefore impact protein stability and activity (8, 9). Met-O can be converted back to Met by methionine sulfoxide reductases (Msrs), which form a large, ubiquitous family of proteins. *S.* Typhimurium expresses four Msrs. Three cytoplasmic enzymes, MsrA, MsrB, and MsrC, cooperate in the reduction of Met-O residues in this compartment, using reducing equivalents provided by the thioredoxin system (10–14). In addition, the biotin sulfoxide reductase BisC participates in Met-O homeostasis in the cytoplasm (15). MsrA, MsrB, and MsrC are important for *S.* Typhimurium virulence in macrophages, mice, and chicken (16, 17). The fourth Msr enzyme, MsrP, a molybdoreductase, repairs HOCl-oxidized proteins in the periplasm, using the membrane-bound MsrQ as a redox partner (18, 19). Whereas MsrP is important for *Campylobacter jejuni* virulence, being involved in chicken colonization, its role in *S.* Typhimurium virulence remains unknown (20).

Author affiliations: [a]Aix-Marseille University, CNRS, Laboratoire de Chimie Bactérienne, Institut de Microbiologie de la Méditerranée, 13402 Marseille, France; [b]Institut de Microbiologie de la Méditerranée, Plate-forme Transcriptomique, 13402 Marseille, France; and [c]de Duve Institute, Université Catholique de Louvain, 1200 Brussels, Belgium

Author contributions: B.E. designed research; C.A., L.L., A.V., R.B., and L.A. performed research; C.A., L.L., A.V., S.G., L.A., J.-F.C., and B.E. analyzed data; and C.A., J.-F.C., and B.E. wrote the paper.

The authors declare no competing interest.

This article is a PNAS Direct Submission.

[1]To whom correspondence may be addressed. Email: ezraty@imm.cnrs.fr.

This article contains supporting information online at https://www.pnas.org/lookup/suppl/doi:10.1073/pnas.2215997120/-/DCSupplemental.

Published March 28, 2023.

The establishment of infection depends on the ability of the pathogen to adapt and resist toxic compounds such as ROS and RCS. Therefore, an in-depth characterization of the antioxidant enzymes expressed by *S.* Typhimurium is required to fully elucidate the adaptation process of this pathogen. Here, we investigated *S.* Typhimurium MsrP in order to identify its role in survival against oxidative stress encountered during mammalian infection and to identify the regulatory pathways controlling its expression.

In the present study, we show that MsrP plays a role in the resistance of *S.* Typhimurium to *N*-chlorotaurine (*N*-ChT), a powerful and bactericidal RCS that results from the reaction between HOCl and taurine, the most abundant free amino acid derivative in the vicinity of neutrophils (21, 22). Moreover, we demonstrate that *N*-ChT induces the two-component CpxRA envelope stress response system (23) and report that *msrPQ* is part of the Cpx regulon. Thus, our work reveals an unexpected link between *N*-ChT oxidative stress and a crucial stress response pathway active in the envelope of *S.* Typhimurium.

Results

MsrP Is Required to Cope with *N*-ChT Stress. Whereas the functional importance of cytoplasmic MsrA and MsrB in the defense mechanisms against oxidative stress is well documented, the role of periplasmic MsrP in this process remains largely unknown. To fill this gap, we investigated the role of *S.* Typhimurium MsrP in the antioxidant defense of this organism. We first assessed whether *msrP* deletion renders *S.* Typhimurium more sensitive to compounds known to generate oxidative stress. In these experiments, we used two ROS [H_2O_2 and $O_2^{\cdot-}$ (the superoxide anion was generated using paraquat)] and two RCS (HOCl and *N*-ChT). We added each compound to the culture during the mid-exponential phase and monitored the growth rates of wild-type (WT) and Δ*msrP* strains. Our results show that deleting *msrP* has no impact on the ability of *S.* Typhimurium to survive exposure to $O_2^{\cdot-}$, H_2O_2, or HOCl at different concentrations (Fig. 1*A* and *SI Appendix*, Fig. S1). Interestingly, however, the *msrP* deletion mutant was more sensitive to *N*-ChT (Fig. 1 *A* and *B*): Δ*msrP* cells indeed need substantially more time to recover from *N*-ChT exposure than WT cells. We observed this phenotype at different concentrations of *N*-ChT (*SI Appendix*, Fig. S1) and could fully rescue the phenotype by complementation with an *msrP*-expressing plasmid (Fig. 1*C*). Furthermore, increasing MsrP levels abrogated the lag phase and rendered the strain more resistant to *N*-ChT compared with the WT. We observed a slight negative effect of the presence of pMsrP plasmid in the stationary phase, most likely due to deregulation of the electron flow in the respiratory chain required for functioning of the MsrPQ system (18). These results indicate that the sensitivity to *N*-ChT exhibited by Δ*msrP* cells is a direct consequence of inactivation of the corresponding gene. Together, these findings indicate that MsrP is involved in the defense mechanisms against *N*-ChT and plays a role in oxidative stress resistance in *S.* Typhimurium.

MsrP Repairs *N*-ChT-Oxidized Proteins. We next explored whether the sensitivity to *N*-ChT resulted from an impaired ability to rescue oxidized proteins in the periplasm of the Δ*msrP* mutant. First, to determine whether *N*-ChT causes Met oxidation in proteins, we treated the model protein calmodulin (CaM) with *N*-ChT and assessed how this treatment impacts CaM migration in sodium dodecyl-sulfate polyacrylamide gel electrophoresis (SDS-PAGE). Indeed, Met-O-containing polypeptides run slower than their reduced counterpart in SDS-PAGE. We observed that CaM exhibited a mobility shift that correlated with the amount of *N*-ChT used (*SI Appendix*, Fig. S2*A*). MsrP treatment was able to reverse this shift (*SI Appendix*, Fig. S2*B*), indicating that *N*-ChT oxidizes proteins by targeting their Met residues. Notably, we observed similar shifts with HOCl but not with H_2O_2 (50 or 100 μM), as previously reported (24).

We sought to obtain direct evidence that *N*-ChT can oxidize periplasmic proteins in vivo and that MsrP is involved in protein-redox control in *S.* Typhimurium. For this purpose, we monitored how *N*-ChT treatment impacts the redox state of the *S.* Typhimurium primary periplasmic chaperone SurA, which is a specific MsrP substrate in *Escherichia coli*. We found that SurA is oxidized by *N*-ChT after 2 h of treatment. Remarkably, whereas the induced expression of MsrP restores the initial mobility of SurA in the WT (~3 h after *N*-ChT exposure, correlating with MsrP expression), SurA remains oxidized and appears to be degraded at 5 h after exposure in the Δ*msrP* mutant (Fig. 1*D*). When the oxidized form of SurA (SurAox) is extracted from *N*-ChT-exposed Δ*msrP* cells and incubated with MsrP in vitro, the initial mobility of SurA is restored (Fig. 1*E*). Collectively, our results support the conclusion that during *N*-ChT stress in *S.* Typhimurium, i) methionine residues in periplasmic proteins are oxidized, and ii) MsrP plays a role in repairing *N*-ChT-oxidized proteins.

Exposure to *N*-ChT Induces MsrP Synthesis. In a previous study, we found that *N*-ChT and HOCl induce *msrP* expression in *E. coli* (25). Therefore, we investigated whether this regulation is conserved in *S.* Typhimurium. For this aim, we monitored MsrP levels by immunoblotting. Our results show a massive accumulation of MsrP after *N*-ChT exposure compared with untreated conditions (Fig. 2*A*), but we did not observe an accumulation after HOCl exposure (*SI Appendix*, Fig. S3). Using a plasmid encoding green fluorescence protein (GFP) under control of the *msrP* promoter, we found that exposure to *N*-ChT increased fluorescence levels by fourfold compared with untreated cells (Fig. 2*B*); importantly, we confirmed that *N*-ChT does not affect GFP fluorescence (*SI Appendix*, Fig. S4). In *E. coli*, RCS up-regulate *msrP* expression via the HprRS two-component system (TCS) (Fig. 2*C*) (25). We hypothesized that the *S.* Typhimurium HprRS-homologous TCS, CopRS, may play a role in the regulation pathway. To test this possibility, we followed MsrP production after *N*-ChT exposure in a Δ*copRS* mutant strain. While MsrP production was abrogated in the *E. coli hprRS* mutant, *N*-ChT exposure induced *msrP* expression in *S.* Typhimurium, irrespective of the presence of the CopRS TCS (Fig. 2*D*). Similarly, we found that expressing a constitutively active variant of HprS (M153A) (25) in *S.* Typhimurium had no impact on MsrP production (*SI Appendix*, Fig. S5). Thus, CopRS is not involved in *msrP* regulation in *S.* Typhimurium, and *N*-ChT induces *msrP* expression in a CopRS-independent manner.

A CpxA Variant Exhibits MsrP Overproduction. The above results suggest that MsrP production is under the control of an unknown *N*-ChT-sensing system in *S.* Typhimurium. Thus, we hypothesized that identifying factors involved in *msrP* regulation may open the way to identify and characterize the *N*-ChT-sensing system. To investigate the *msrP* regulation pathways in *S.* Typhimurium, we designed a genetic screen to search for MsrP-overproducer variants conferring greater Met-O-reducing capacity. For this purpose, we took advantage of a methionine auxotroph mutant lacking all cytoplasmic Msrs and BisC (Δ*metA* Δ*3msr*^{cyto}Δ*bisC*) and selected suppressors by performing a growth assay on minimal media containing Met-O (Fig. 3*A*), as reported by Gennaris et al. (18). This approach allowed us to isolate strain LLS662, which

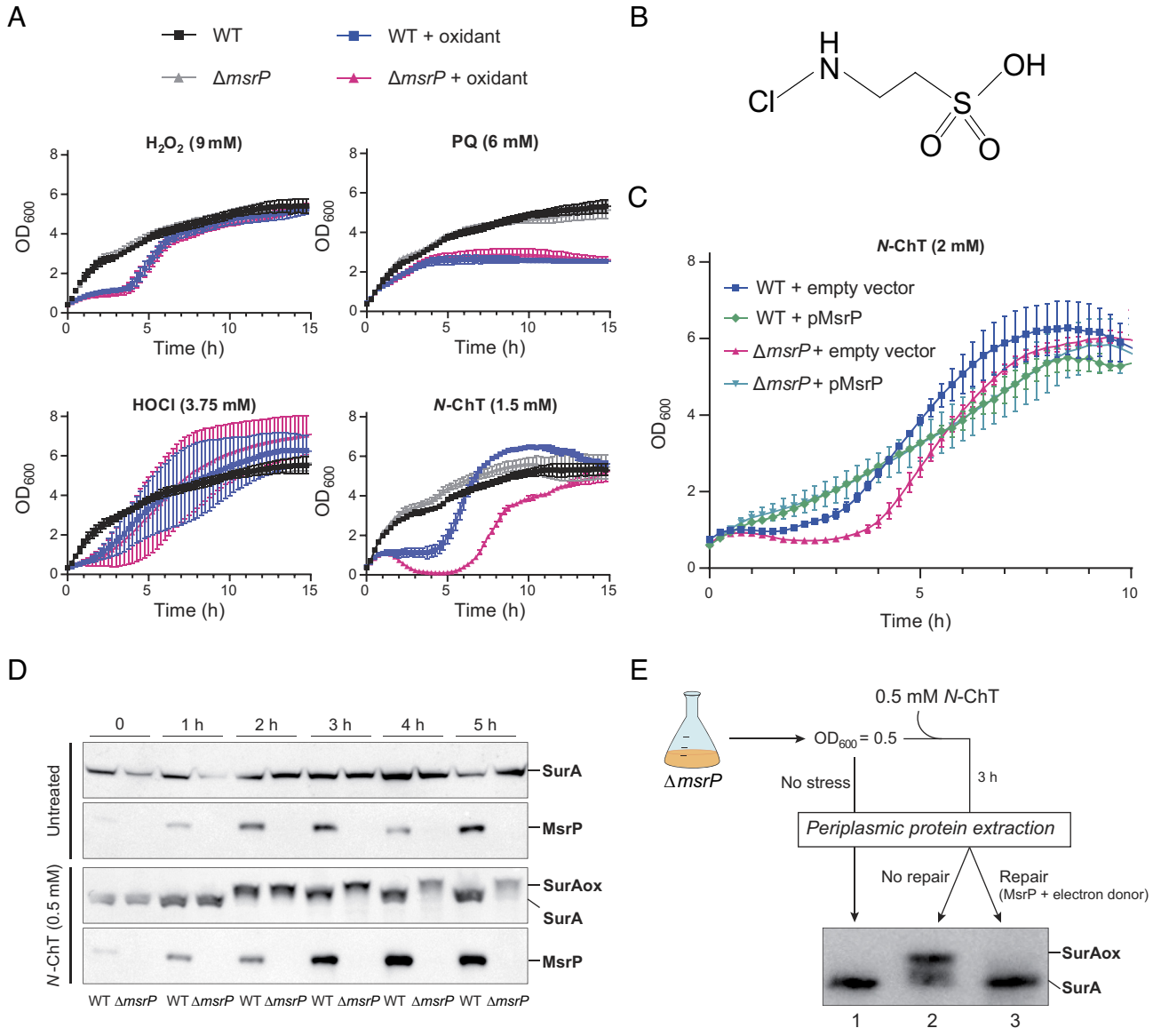

Fig. 1. *msrP* is required for *N*-ChT resistance of *S.* Typhimurium. (*A*) Growth of WT and Δ*msrP* (LA575) strains was monitored by OD_{600} over time using a microplate reader. Cells were grown in flasks of LB at 37 °C to an OD_{600} of 0.5. At this point, 130 µL of culture was distributed to each well in a 96-well microplate, and 20 µL of oxidant was added to the cells to reach a final concentration leading to a growth defect [paraquat (PQ): 6 mM, H_2O_2: 9 mM, HOCl: 3.75 mM, *N*-ChT: 1.5 mM]. Growth was monitored in each well with an absorbance of approximately 0.5 at t = 0. Error bars indicate the SDs of biological replicates, *n* = 6. (*B*) Diagram of the structure of *N*-ChT. (*C*) Growth of the WT strain carrying an empty vector (pJF119EH) or pMsrP (pAC001) plasmid and Δ*msrP* strains carrying an empty vector or pMsrP plasmid, which overproduced MsrP, was monitored by OD_{600} for 10 h. At t = 0, *N*-ChT (2 mM) was added using the same procedure described in (*A*). Error bars indicate the SDs of biological replicates, *n* = 4. (*D*) WT and Δ*msrP* (LA575) cells were grown in LB at 37 °C. At an OD_{600} of 0.5, cells remained untreated or were treated with *N*-ChT (0.5 mM), and SurA and MsrP proteins were analyzed by immunoblotting over 5 h. *N*-ChT treatment leads to the appearance of SurAox, exhibiting a mobility shift on SDS-PAGE resulting from Met-O formation. This blot is representative of three independent experiments. (*E*) Δ*msrP* (LA575) cells were grown in LB at 37 °C. At an OD_{600} of 0.5, cells remained untreated or were treated for 3 h with *N*-ChT (0.5 mM). Periplasmic extracts were prepared and then remained untreated or were reduced by incubation with MsrP in presence of an electron donor. The SurA protein form was analyzed by immunoblotting.

grows substantially faster on minimal medium containing Met-O than its parental strain (Fig. 3*B*). Whole-genome sequencing of strain LLS662 revealed a deletion of six nucleotides within the *cpxA* gene, causing the deletion of two amino acids in CpxA, the histidine kinase of the Cpx system (Fig. 3*C*); we refer to the CpxA variant as CpxA*. We found that CpxA* expression causes a ~100-fold increase in *msrP* messenger RNA (mRNA) levels in strain LLS662 compared with the parental strain. Accordingly, we measured higher *msrP-gfp* expression and elevated MsrP protein levels (Fig. 3*D*). CpxA is the sensor of the envelope stress response (CpxRA TCS), in which CpxR is the response regulator. To further investigate whether MsrP overproduction in LLS662 occurs via the CpxRA pathway, we deleted *cpxR* in the suppressor strain (strain LLS672, a derivative of LLS662 that does not contain the CmR cassette), which prevented its growth on Met-O and restored WT expression levels of *msrP* (Fig. 3 *B* and *D*). Moreover, we found that artificial activation of CpxRA by overproduction of the lipoprotein NlpE (26) allowed Δ*metA* Δ*3msr*^{cyto}Δ*bisC* to grow on M9-Met-O medium and led to overproduction of MsrP (*SI Appendix*, Fig. S6 *A* and *B*). Finally, deletion of *msrP* prevented LLS672 from growing on Met-O (Fig. 3*B*). Together, these results indicate that the CpxRA signaling pathway modulates the expression of *msrP*.

CpxR Binds the *msrP* Promoter Region. Next, we investigated whether CpxR can act directly on the *msrP* promoter region.

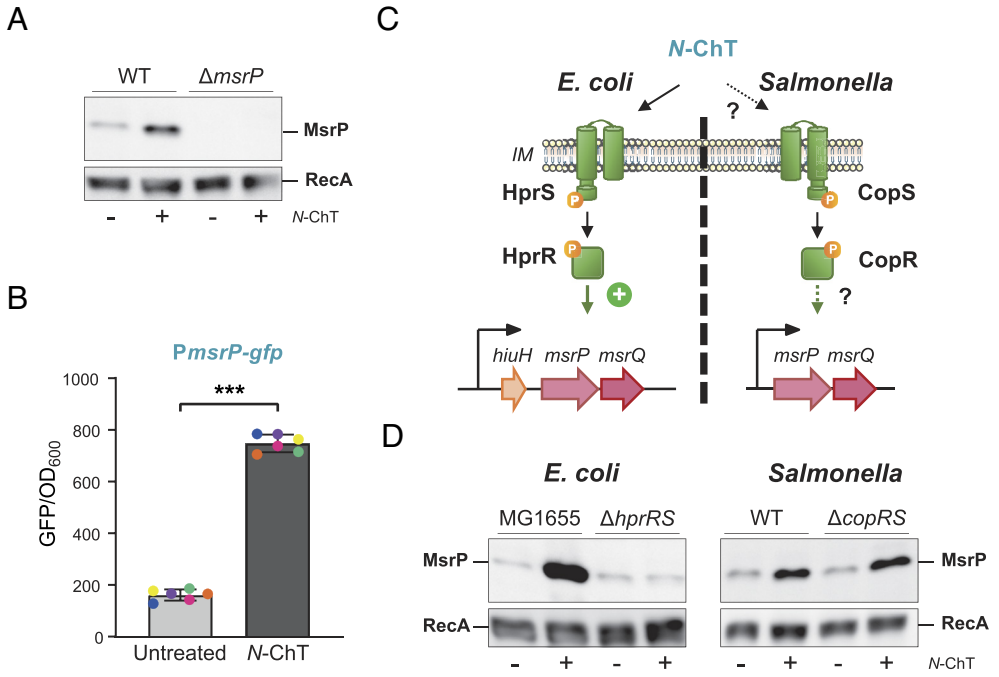

Fig. 2. *N*-ChT activates the expression of *msrP*. (*A*) WT and Δ*msrP* (LA575) cells were grown in LB at 37 °C. At an OD_{600} of 0.5, cells remained untreated or were treated for 1 h with *N*-ChT (1 mM). Immunoblot analysis shows that *N*-ChT induces MsrP synthesis in the WT strain. RecA was used as an internal loading control stained on the same blot. This blot is representative of three independent experiments. (*B*) The *msrP* promoter was fused to *gfp*, yielding the p*msrP-gfp* (pLA192) vector. Liquid cultures of the strain carrying the *msrP-gfp* fusion were treated at an OD_{600} of 0.5 with 1 mM *N*-ChT. OD_{600} and fluorescence were measured 4 h after the application of stress. Error bars indicate the SDs of biological replicates, $n = 6$. Statistical analysis was performed using Student's *t* test (***$P \leq 0.001$). (*C*) Schematic model of *msrP* induction by *N*-ChT via (*Left*) the HprRS TCS in *E. coli* and (*Right*) the homologue CopRS TCS in *S.* Typhimurium. (*D*) Immunoblot analysis showing that *N*-ChT induces MsrP synthesis in the WT strain (MG1655) but not in Δ*hprRS* (LL1085) in *E. coli* (*Left*). RecA was used as an internal loading control stained on the same blot. Immunoblot analysis shows that *N*-ChT induces MsrP synthesis in the WT and Δ*copRS* (LA604) strains in *S.* Typhimurium (*Right*). These blots are representative of three independent replicates.

First, an in silico analysis of the *msrP* promoter region identified a putative CpxR-binding site (5′-GATAAAN$_5$GTCAC-3′) between positions −71 and −87, relative to the transcription start site (Fig. 3*E*). We then purified the CpxR protein and performed an electrophoretic mobility shift assay (EMSA) using *msrP* promoter DNA and nonspecific DNA as a potential competitive substrate. Migration of the *msrP* promoter slowed in the presence of CpxR in a dose-dependent manner. In these experiments, we used the *cpxP* promoter, which is known to interact directly with CpxR, as a positive control (Fig. 3*F*). By comparing shifts obtained with both promoters, we demonstrated the specificity of CpxR binding to the *msrP* promoter. Thus, we conclude that CpxR directly binds the *msrP* promoter, suggesting that the CpxRA TCS controls *msrP* expression.

N-ChT Is a Signal for the CpxRA Pathway. The CpxRA system, which has been intensively studied, is traditionally associated with envelope protein quality control. CpxA senses a diverse number of stresses, including increased osmolarity, elevated pH, perturbations in peptidoglycan synthesis, defects in lipoprotein trafficking, and exposure to copper or antibiotics such as gentamicin. Therefore, it is thought that CpxRA activation protects the cell envelope under these harmful circumstances. While ROS can be associated with copper stress, a well-known Cpx activator (28–33), researchers have not yet reported a direct connection between the CpxRA system and ROS or RCS. Because *N*-ChT, a physiological RCS, induces *msrP* expression, we hypothesized that a previously unknown function of CpxRA could be to monitor the RCS *N*-ChT in the envelope. To test this hypothesis, we determined how *N*-ChT exposure impacts both *msrP* expression (using the *msrP-gfp* fusion) and MsrP production in Δ*cpxR* cells, in which the Cpx TCS cannot be activated. We found that *cpxR* deletion makes the strain more sensitive to *N*-ChT (*SI Appendix*, Fig. S7) and prevents both the activation of *msrP* expression and MsrP accumulation following treatment with *N*-ChT (Fig. 4 *A* and *B*). Moreover, using a *cpxP-gfp* transcriptional fusion whose expression is CpxR-dependent (34), we observed increased *cpxP-gfp* expression levels in the presence of *N*-ChT in the WT strain but not in the Δ*cpxR* mutant (Fig. 4*C*). Notably, the expression levels of the *cpxP-gfp* fusion remained unchanged when cells were exposed to H_2O_2 or paraquat and showed only a moderate change upon exposure to HOCl (*SI Appendix*, Fig. S8). Thus, Cpx is activated by *N*-ChT in *S.* Typhimurium.

Because Cpx has primarily been studied in *E. coli*, we investigated the impact of *N*-ChT on Cpx in this organism. We measured increased *cpxP-lacZ* expression in WT but not Δ*cpxR* cells upon *N*-ChT treatment, indicating that the ability of Cpx to respond to this RCS agent is conserved in *E. coli* (*SI Appendix*, Fig. S9*A*). However, in this organism, deletion of *cpxR* had no impact on MsrP expression following *N*-ChT treatment (*SI Appendix*, Fig. S9*B*), demonstrating that *msrP* is not part of the Cpx regulon in *E. coli*.

N-ChT Triggers Cpx in an NlpE-Dependent Manner. Finally, we sought to identify the molecular signal that induces Cpx when *S.* Typhimurium is exposed to *N*-ChT. A recent report demonstrated that Cpx is activated when maturation of the *E. coli* outer membrane (OM) lipoprotein NlpE is perturbed by copper, a redox-active metal (31). Therefore, we hypothesized that NlpE may also play a role in Cpx activation in *S.* Typhimurium. To test this hypothesis, we monitored MsrP production during *N*-ChT stress in Δ*nlpE* cells; we found that deleting *nlpE* significantly

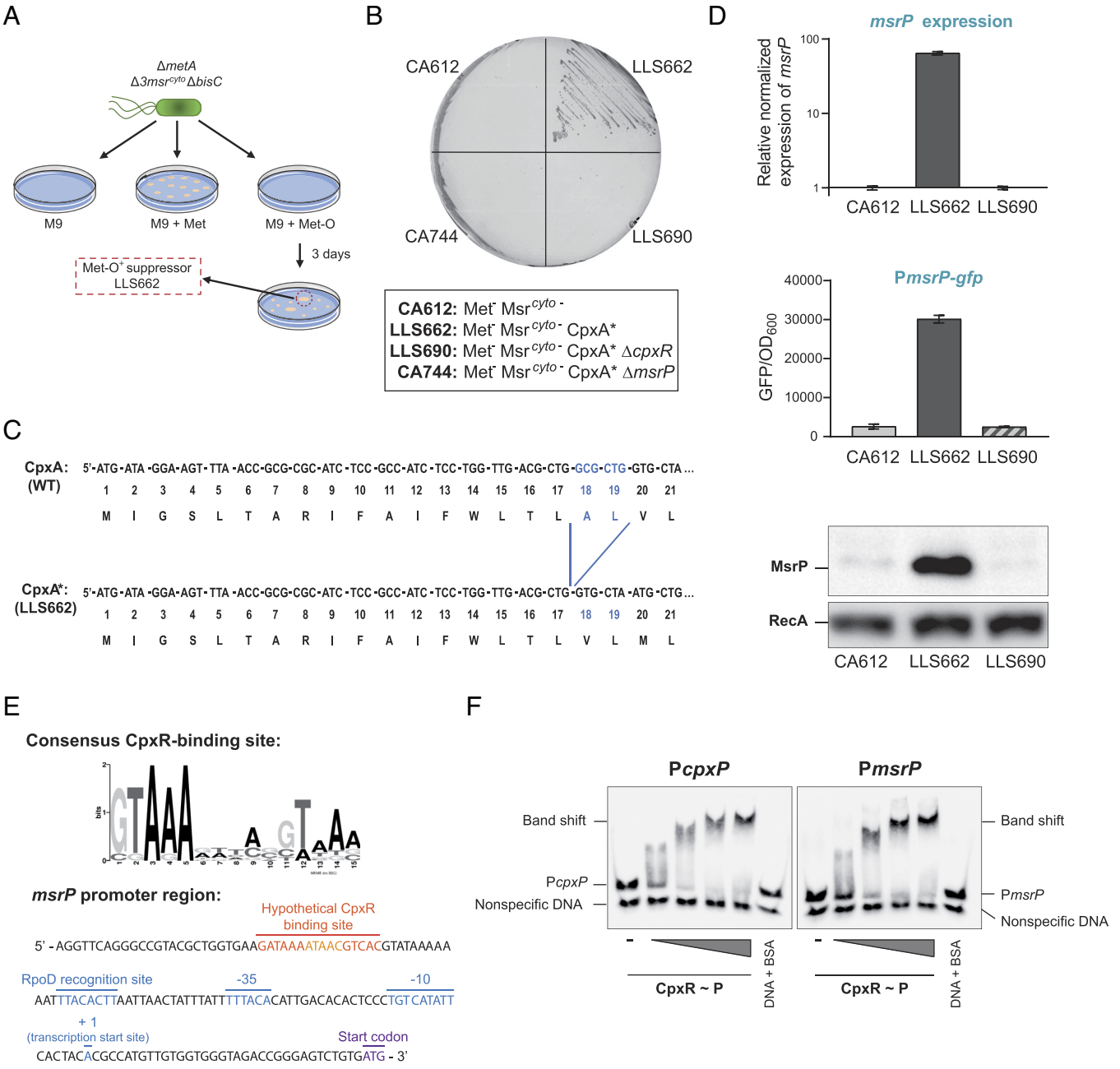

Fig. 3. CpxRA signaling pathway modulates the expression of *msrP*. (*A*) Schematic model of the genetic screen used to search for MsrP-overproducing suppressor variants conferring higher Met-O-reducing capacity. A methionine auxotroph mutant lacking all cytoplasmic Msrs [denoted as Δ*metA* Δ3*msr*^{cyto}Δ*bisC* (CA612)] can use Met but not Met-O to grow on M9 minimal medium. The Met-O+ suppressor LLS662 was isolated on minimal medium containing Met-O after 3 d. (*B*) Cells were streaked onto M9 minimal medium plates supplemented with Met-O and incubated at 37 °C for 3 days. The parental strain CA612 (Δ*metA* Δ3*msr*^{cyto}Δ*bisC*) did not grow on Met-O as the only Met source in contrast to suppressor LLS662. Deletion of *cpxR* (LL690) or *msrP* (CA744) prevents growth on Met-O. This image is representative of three independent experiments. (*C*) Comparison of the DNA and protein sequences of CpxA in the WT and LLS662 strains. (*D*) *msrP* is up-regulated in the LLS662 strain. An increase was observed at the i) mRNA level by RT-qPCR (*Top*), ii) transcriptional level by the *msrP-gfp* fusion (*Middle*), and iii) protein level by immunoblot analysis (*Bottom*). RecA was used as an internal loading control stained on the same blot. Deletion of *cpxR* prevents *msrP* upregulation. (*E*) *Top*: Consensus sequence logo of the CpxR-binding site in *S.* Typhimurium adapted from Subramaniam et al. (27) using MEME (Multiple Em for Motif Elicitation) software. *Bottom*: In silico analysis of the *msrP* promoter region performed by BPROM (SoftBerry), showing a putative CpxR-binding site in orange (5′-GATAAAN$_5$GTCAC-3′) between positions −71 and −87. The RpoD recognition site and the transcription start site are represented in blue and the start codon in purple. (*F*) Results of EMSA experiments with increasing concentrations of phosphorylated CpxR with the *cpxP* (*Left*) and *msrP* (*Right*) promoters. Bovine Serum Albumin (BSA) was incubated with both promoters as a negative control (far right lanes). These gels are representative of three independent experiments.

reduced MsrP expression levels compared with the WT (Fig. 4*A*) and inhibited the induction of *msrP-gfp* fusion and *cpxP-gfp* fusion (Fig. 4 *B* and *C*). In addition, Δ*nlpE* cells were slightly more sensitive to *N*-ChT (*SI Appendix*, Fig. S7). These results indicate that NlpE likely participates in Cpx activation during *N*-ChT stress in *S.* Typhimurium.

It has been proposed that copper blocks the maturation of NlpE and other lipoproteins by binding to their N-terminal cysteine residue (31), which is normally lipidated. As a result, NlpE accumulates in the inner membrane (IM), where it induces Cpx by interacting with CpxA (26). Thus, we hypothesized that exposing *S.* Typhimurium cells to *N*-ChT may impact lipoprotein transport. Researchers commonly use Lpp, the most abundant OM lipoprotein, as a read-out for lipoprotein maturation: alterations in this process, such as those caused by copper or specific inhibitors of the lipoprotein maturation process (31), lead to the accumulation of

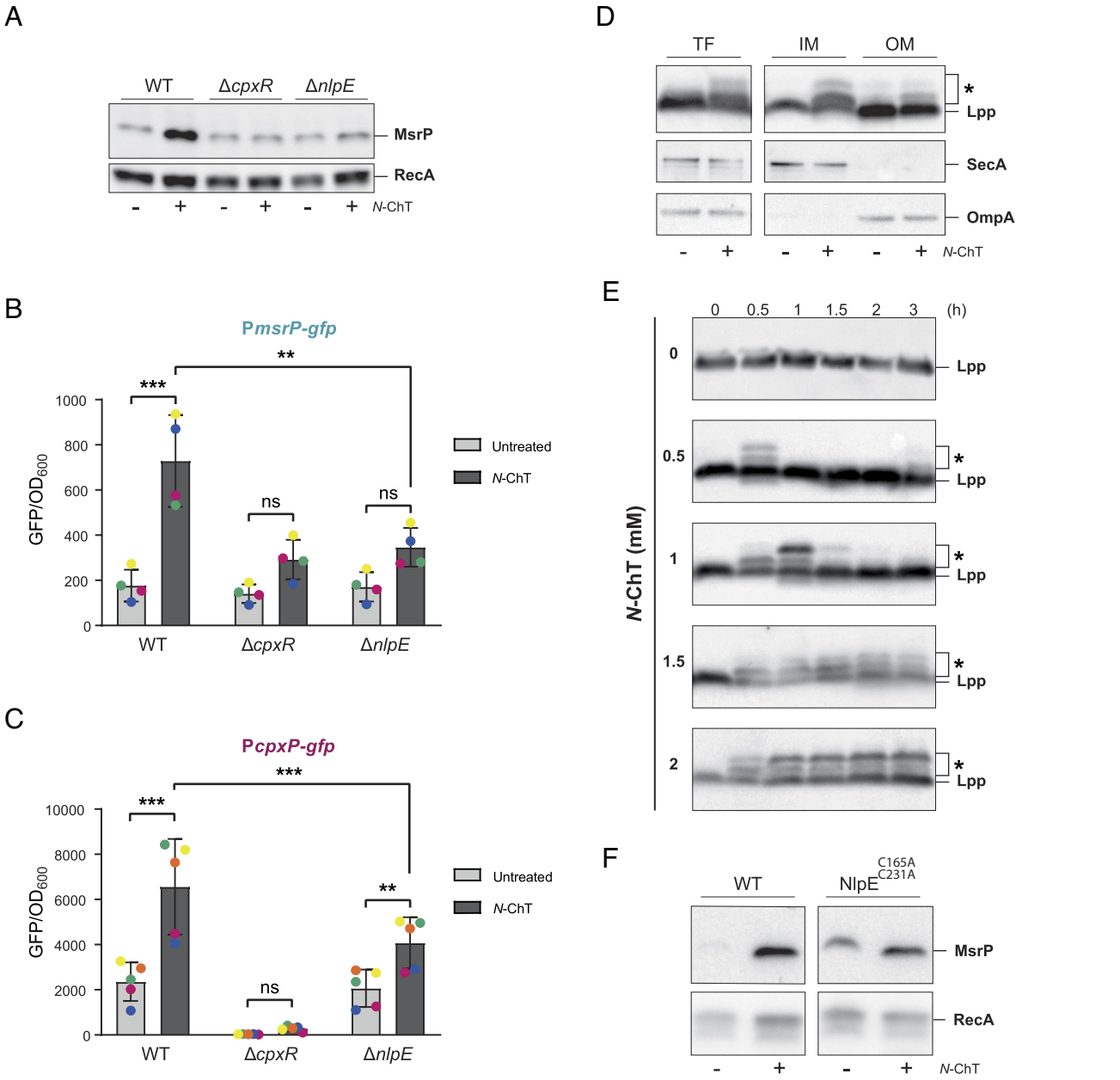

Fig. 4. *N*-ChT disrupts the lipoprotein NlpE, which participates in the activation of CpxRA. (*A*) WT, Δ*cpxR*, and Δ*nlpE* cells were grown in LB at 37 °C. At an OD_{600} of 0.5, cells remained untreated or were treated for 1 h with *N*-ChT (1 mM). Immunoblot analysis measured MsrP synthesis in the WT, Δ*cpxR*, and Δ*nlpE* strains. RecA was used as an internal loading control stained on the same blot. The blots are representative of three independent experiments. (*B*) WT, Δ*cpxR* (LL663), and Δ*nlpE* (CA689) strains carrying the *msrP-gfp* fusion were grown in LB at 37 °C. At an OD_{600} of 0.5, cells remained untreated or were treated with 1 mM *N*-ChT. OD_{600} and fluorescence were measured 4 h after treatment. Error bars indicate the SDs of biological replicates, $n = 4$. Statistical analysis was carried out by two-way ANOVA with Tukey's multiple-comparison test (***$P \leq 0.001$; **$P \leq 0.01$; ns, not significant). (*C*) The *cpxP* promoter was fused to *gfp*, yielding the p*cpxP-gfp* (pLA197) vector. Liquid cultures of the strains containing the *cpxP-gfp* fusion were treated at an OD_{600} of 0.5 with 1 mM *N*-ChT. OD_{600} and fluorescence were measured 4 h after the application of stress. Error bars indicate the SDs of biological replicates, $n = 5$. Statistical analysis was performed by two-way ANOVA with Tukey's multiple-comparison test (***$P \leq 0.001$; **$P \leq 0.01$; ns, not significant). (*D*) Subcellular localization of lipoprotein Lpp after *N*-ChT stress. WT cells were grown in LB at 37 °C. At an OD_{600} of 0.5, cells remained untreated or were treated for 0.5 h with *N*-ChT (1 mM). Cell fractionation was carried out, and immunoblot analysis was performed on the total fraction (TF), inner membrane (IM), and outer membrane (OM). Antibodies against OmpA (OM) and SecA (IM) were used as membrane purity controls. The blot is representative of three independent experiments. (*E*) WT cells were grown to an OD_{600} of 0.5. At this point, *N*-ChT was added at different concentrations (0.5, 1, 1.5, and 2 mM), and cell extracts were removed every 30 min over 3 h and probed for Lpp by immunoblotting. Adding *N*-ChT leads to the appearance of additional Lpp (noted Lpp*) forms with higher apparent molecular weights. The blots are representative of three independent experiments. (*F*) WT and *nlpE:nlpE*$_{C165AC231A}$ (LLS749) cells were grown in LB at 37 °C. At an OD_{600} of 0.5, cells remained untreated or were treated for 1 h with *N*-ChT (1 mM). Immunoblot analysis measured MsrP synthesis in the WT and *nlpE:nlpE*$_{C165AC231A}$ strains. RecA was used as an internal loading control stained on the same blot.

Lpp intermediates in the IM. We found that exposing *S.* Typhimurium to *N*-ChT causes a slight accumulation of Lpp in the IM (Fig. 4*D*). In addition, Lpp species migrating with higher apparent molecular masses appear in membrane extracts from *N*-ChT-treated cells (Fig. 4*D*), regardless of the presence of MsrP (*SI Appendix*, Fig. S10). Slowly migrating species are often indicative of Lpp maturation defects (31); although the bands observed here appear to be different from those previously reported for cells treated with copper [*SI Appendix*, Fig. S11; (31)], their formation indicates that Lpp is impacted by *N*-ChT. Moreover,

whereas low *N*-ChT concentrations led to a transient appearance of species with a higher apparent molecular weight (0.5 to 1 h), the accumulation was permanent when higher concentrations were used (Fig. 4*E*). Another model has been put forward to explain how NlpE activates Cpx. In this model, cysteine residues in the C-terminal domain—NlpE contains four cysteine residues involved in two disulfide bonds, one in the N-terminal domain, one in the C-terminal domain—function as a sensor for redox perturbations (26). We thus also considered the possibility that the C-terminal cysteines could be important for *N*-ChT detection and Cpx activation. To assess this possibility, we performed site-direct mutagenesis with Cys-to-Ala ($nlpE_{C165AC231A}$) substitutions. Interestingly, expression of $NlpE_{C165AC231A}$ from the native *nlpE* locus constitutively increased MsrP production (by approximately fourfold) (Fig. 4*F*) in a CpxR-dependent manner (*SI Appendix*, Fig. S12). *N*-ChT treatment further increased MsrP production (Fig. 4*F*), although less than in the WT. Altogether, these results indicate that *N*-ChT activates the Cpx pathway in an NlpE-dependent manner; two mechanisms—defects in lipoprotein maturation (Fig. 4*D*) and redox sensing (Fig. 4*F*)—can be envisaged to govern this behavior. These two potential mechanisms are not necessarily mutually exclusive.

Discussion

Here, we investigated the role of *S.* Typhimurium MsrP during oxidative stress. We found that the Cpx stress response activates *msrP* expression in response to *N*-ChT, an RCS that is able to oxidize Met residues. We showed that MsrP is required to cope with *N*-ChT, conferring a central role to this enzyme in the resistance to RCS stress in *S.* Typhimurium. Importantly, our work i) shows that *msrP* transcription in *S.* Typhimurium is controlled differently than in *E. coli*, ii) identifies *msrP* as a member of the *S.* Typhimurium Cpx regulon, and iii) shows that *N*-ChT triggers Cpx in an NlpE-dependent manner. Our data establish an unexpected link between *N*-ChT oxidative stress and an envelope stress response.

During mammalian infection, pathogens experience oxidative stress, leading to the oxidation of cellular macromolecules, including proteins. The importance of cytoplasmic oxidized-protein repair processes in oxidative stress resistance and virulence in *S.* Typhimurium is well documented (16, 17, 35) Here, our results show that an *S.* Typhimurium mutant strain lacking the periplasmic enzyme MsrP is hypersensitive to *N*-ChT. Given that *N*-ChT is an RCS produced from HOCl and taurine by neutrophils (21, 22) recruited to the site of infection to clear *S.* Typhimurium, this result suggests that MsrP could participate in *S.* Typhimurium pathogenesis. Thus, the activity of all Msrs allows *S.* Typhimurium to resist the oxidative stress produced by neutrophils. A dedicated study on the importance of MsrP in *S.* Typhimurium virulence is needed to obtain a complete, global view of Met-O homeostasis during infection.

Originally, researchers discovered the MsrPQ repair system in *E. coli* based on a hit suppressor on the *hprS* gene (18). In *E. coli*, the *hprRS* operon is upstream and in the opposite direction of the *hiuH-msrPQ* operon. The *S.* Typhimurium CopRS TCS is defined as an HprRS homologue based on the close vicinity of the *copRS* and *hiuH* genes in the genome organization. Here, by monitoring MsrP production, we established that the CopRS system is not involved in *msrP* regulation. However, using a genetic screen similar to the previous screen used in *E. coli*, we revealed the involvement of another TCS, the CpxRA system. Therefore, it appears that both *enterobacteriacea* use the same strategy (i.e., a TCS) to regulate *msrP*, but via different pathways. Strikingly, we found that the signals capable of inducing *msrP* expression differ between *S.* Typhimurium and *E. coli*. Indeed, a previous work reported that RCS (HOCl and *N*-ChT) mediate *msrP* expression in *E. coli* (25), whereas this study showed that only *N*-ChT leads to a response in *S.* Typhimurium. This difference can be explained by the nature of the membrane sensor involved in stress detection: Activation of the HprS sensor depends on a direct Met-redox switch within the periplasmic loop (25) while CpxA activation arises from lipoprotein maturation disruption and possibly periplasmic protein aggregation (26, 31, 36). In contrast to HOCl, *N*-ChT is a long-lived RCS with weak membrane-diffusion action (21, 37). We can assume that the poor membrane permeability of *N*-ChT provides a better signal for CpxA by damaging more elements of the periplasm than the highly diffusible HOCl.

The precise physiological concentration range of *N*-ChT in close proximity to pathogens remains unknown. However, previous studies have detected *N*-ChT concentrations ranging from 10 to 50 μM in the supernatants of activated granulocytes (21, 22, 38). Given the limited membrane permeability of *N*-ChT, it is reasonable to conclude that bacteria within a phagosome would likely be exposed to *N*-ChT concentrations higher than these values. Thus, we can reasonably infer that the molecular mechanism highlighted in our study is biologically relevant.

A recent study identified the Cpx regulon in *S.* Typhimurium using a global transcriptomic analysis and found that approximately 400 genes are differentially regulated (27). The study identified STM3377 and STM3378, which we now know correspond to the *msrP* and *msrQ* genes, respectively, as highly up-regulated in a Δ*cpxA* strain. The authors did not attempt to add both genes in the Cpx regulon due to the absence of a CpxR-consensus-binding motif within the operon promoter. However, our EMSA data reveal that CpxR binds the *msrP* promoter with high efficiency. The comparison of CpxR binding affinity on *msrP* and *cpxP* promoters is in accordance with a previous transcriptomic analysis showing that both genes are among the first hits induced by CpxR (27). Further experiments are needed to identify the CpxR-binding motif within the *msrP* promoter. A comparative analysis shows the presence of a species-specific Cpx response. In view of our work, considering that MsrP is a molybdoenzyme that translocates across the IM via the twin-arginine translocation system (*tatABCD*), it is interesting to note that the *tatABCD* operon is a direct CpxR target in *S.* Typhimurium, in contrast to the constitutive expression observed in *E. coli* (27, 39). Likewise, we note that the molybdenum transporter ModABC system in *S.* Typhimurium appears to be up-regulated in a Cpx-dependent manner (27). Therefore, in *S.* Typhimurium, increasing the efficiency of periplasmic protein translocation and molybdenum uptake would facilitate MsrP maturation. In *S.* Typhimurium, the major envelope oxidoreductase DsbA, which introduces disulfide bonds in periplasmic proteins, and the *S.* Typhimurium-specific disulfide folding machinery in the periplasm, ScsABCD, are Cpx regulon members (27, 33, 40). Adding *msrPQ* as a direct target of Cpx shows that maintaining methionine and cysteine redox control during envelope stress is a crucial process.

Researchers have proposed numerous cues for activation of the Cpx envelope stress response, including exogenous stresses such as alkaline pH, high osmolarity, copper, gentamicin, and drugs targeting peptidoglycan synthesis (31, 41–45). While copper stress can be associated with ROS, here, we report that *N*-ChT oxidative stress elicits a direct Cpx response. This result provides a role for the Cpx pathway in the oxidative stress response of *S.* Typhimurium. However, the link seems to be quite specific for *N*-ChT, as HOCl, H_2O_2, and the $O_2^{\cdot-}$ generator paraquat were unable to activate Cpx. Thus, in *S.* Typhimurium, Cpx appears to be part of an RCS-specific responsive

pathway in addition to the characterized HOCl-specific transcription factor HypT (46). We also report that the lipoprotein NlpE is involved in Cpx activation by *N*-ChT. Although our results allow us to discuss two potential activation mechanisms, further research is required to fully elucidate how NlpE triggers Cpx at the molecular level. It will also be interesting to determine what causes the formation of the slowly migrating Lpp species. Interestingly, LppA and LppB of *S.* Typhimurium have only one methionine residue in their sequence; thus, the findings that several Lpp bands migrate with higher molecular masses and that the formation of these bands does not depend on the presence of MsrP (*SI Appendix*, Fig. S10) suggest that methionine oxidation does not play a role in the formation of the modified Lpp species. Furthermore, the fact that one of the Lpp* bands is also detected in the OM (Fig. 4*D*) suggests that this band may not result from maturation defects. Additional experiments, including mass spectrometry analysis, are needed to clarify this point.

In conclusion, this study has shown that *S.* Typhimurium uses the Cpx TCS to detect *N*-ChT in an NlpE-dependent manner, which consequently promotes the repair of periplasmic oxidized proteins.

Materials and Methods

Strains and Microbial Techniques. *SI Appendix*, Tables S1 and S2 present the strains and primers, respectively, used in this study.

We used *Salmonella* ser. Typhimurium ATCC14028 as the WT strain. We performed gene deletions using the one-step λ Red recombinase chromosomal inactivation system (47). Deletions were transferred to the WT using P22 transduction procedures and were verified by PCR (primers listed in *SI Appendix*, Table S2). To excise the resistance cassette when required, we used pCP20 (47). In each experiment, we used 3 to 4 colonies to inoculate overnight cultures in lysogeny broth (LB) (or M9 minimal medium when specified) to ensure culture heterogeneity. We grew the cultures aerobically overnight at 37 °C with agitation and then diluted the cultures 1:100 in the appropriate medium. We applied antibiotics for plasmid maintenance when appropriate at the following concentrations: 100 μg mL^{-1} ampicillin, 25 μg mL^{-1} chloramphenicol, 100 μg mL^{-1} kanamycin, and 100 μg mL^{-1} spectinomycin.

***N*-ChT Synthesis.** *N*-ChT (Cl-HN-CH_2-CH_2-SO_3^-) was produced by the reaction between a solution of 100 mM HOCl (Honeywell) and 100 mM taurine (Sigma-Aldrich) in 0.1 M phosphate potassium buffer (pH 7.4). After 10 min at room temperature, we determined the *N*-ChT concentration by measuring the absorbance at 252 nm ($\varepsilon = 429\ M^{-1}\ cm^{-1}$) and stored the medium at 4 °C.

Identification of a Suppressor Variant Conferring Met-O-Reducing Capacity by MsrP Overproduction. To search for an MsrP-overproducing suppressor variant conferring greater Met-O-reducing capacity, we grew CA612 (Δ*metA* Δ*3msr*^{cyto}Δ*bisC*) aerobically overnight in M9 minimal medium supplemented with 0.2% casamino acids (Gibco) at 37 °C. After 16 h of growth, we washed the cells with phosphate-buffered saline (PBS) and spread 100 μL culture onto M9 minimal medium plates supplemented with Met-O (20 μg mL^{-1}). Plates were incubated at 37 °C for 3 days. We isolated the resulting colonies on LB plates. To verify that the suppressors were still auxotrophic for methionine, we streaked the suppressors on M9 minimal medium plates. Then, MsrP levels were determined by immunoblotting, as described below. To sequence the genome of the obtained suppressor, LLS662 (*cpxA**), we isolated the genomic DNA as described previously (48). DNA fragmentation via a Covaris instrument (M220 Focused Ultrasonicator) followed by library construction using the NEBNext Ultra II DNA Library Prep Kit led to 350-bp insert size libraries. Paired-end reads (2 × 150 bp) were sequenced on an Illumina MiSeq platform. After read cleaning (Trimmomatic v0.39), we performed variant calling using Snippy (v4.3.6; https://github.com/tseemann/snippy) referring to the genome sequence GCF_000022165 (National Center for Biotechnology Information).

Fluorescence Quantification with a Microplate Reader. WT cells harboring p*msrP-gfp* or p*cpxP-gfp* grew aerobically in LB supplemented with ampicillin at 37 °C for approximately 2 h (corresponding to four cell-doubling cycles) until an OD_{600} of 0.5 was reached. From these cultures, 130 μL was distributed to wells in a 96-well flat-bottom black microplate (Greiner Bio-One). We prepared oxidants in 0.1 M phosphate potassium buffer (pH 7.4) and added 20 μL to the wells to obtain the following final concentrations: 1 mM *N*-ChT, 0.5 mM paraquat (Sigma-Aldrich), 2 mM H_2O_2 (Honeywell), 1 mM HOCl (Honeywell), 2 mM $CuSO_4$ (Sigma-Aldrich). Results correspond to values obtained at 4 h after the addition of stress.

To evaluate *msrP* expression in CA612 (Δ*metA* Δ*3msr*^{cyto}Δ*bisC*), LLS662 (*cpxA**), and LLS690 (*cpxA** Δ*cpxR*), we transformed cells with p*msrP-gfp* and grew cultures aerobically overnight in LB supplemented with ampicillin at 37 °C. After 16 h of growth, cultures were transferred to wells of a 96-well flat-bottom black microplate (Greiner Bio-One).

We analyzed the fluorescence using a Spark microplate reader (TECAN) with excitation and emission wavelengths of 482 and 515 nm, respectively. Fluorescence values were divided by the absorbance at 600 nm to obtain values that were proportional to the bacterial cell concentration. Graphs were prepared using Prism 8 (GraphPad Software, Inc.).

In Vitro Oxidation of CaM. We treated CaM (6 μM) with 50 and 100 μM oxidant, corresponding to one and two molar equivalents of methionine, respectively, for 30 min at 37 °C. Each sample was suspended in Laemmli SDS sample buffer and heated for 10 min at 95 °C. We resolved the samples on a 17% Tris-glycine SDS-PAGE gel at 125 V for 2.5 h and stained the gel with Coomassie blue. We performed the repair of oxidized CaM by MsrP as described previously, using 10 mM benzyl viologen and 10 mM sodium dithionite at 37 °C for 1 h (18).

In Vivo Analysis of SurA Oxidation after *N*-ChT Exposure by Gel Shift Assays. WT and LA575 (Δ*msrP*) cells grew aerobically in LB at 37 °C for approximately 2 h (corresponding to approximately four cell-doubling cycles) until an OD_{600} of 0.5 was reached. At this point, we split the cultures and added *N*-ChT (0.5 mM) for one condition. Before the addition of *N*-ChT (t = 0) and at different time points (t = 1 h, 2 h, 3 h, 4 h, and 5 h), equivalent cell densities (normalized by A_{600}) were pelleted by centrifugation (3,000 g, 5 min). Samples were suspended in Laemmli SDS sample buffer and heated for 10 min at 95 °C. We resolved the samples on a 12% NuPAGE Bis-Tris gel (Invitrogen) at 125 V for 2.5 h. For immunoblot analysis, we transferred the resolved proteins to 0.2-μm nitrocellulose membranes, which we then probed with anti-SurA antibody [provided by the Jean-François Collet Lab, de Duve Institute, Université Catholique de Louvain (UCLouvain)], followed by a horseradish peroxidase (HRP)-conjugated anti-rabbit IgG secondary antibody (Promega). We imaged the chemiluminescence signals using an ImageQuant Las4000 camera (GE Healthcare). We performed the repair of oxidized SurA by MsrP as described previously, using 10 mM benzyl viologen and 10 mM sodium dithionite at 37 °C for 1 h (18).

Immunoblot Analysis of MsrP Production. To determine MsrP levels after *N*-ChT exposure in *S.* Typhimurium, we grew cultures aerobically in LB at 37 °C until an OD_{600} of 0.5 was reached. At this point, we split the cultures into two subcultures and added *N*-ChT (1 mM) to one tube. After 1 h, we prepared the samples for immunoblot analysis.

To determine MsrP levels after *N*-ChT exposure in *E. coli*, we grew MG1655 and LL1085 (Δ*hprRS*) cells aerobically in LB at 37 °C until an OD_{600} of 1 was reached. We then split the cultures into two subcultures and added *N*-ChT (1 mM) to one tube. After 2.5 h, we prepared the samples for immunoblot analysis.

To determine MsrP levels in CA612 (Δ*metA* Δ*3msr*^{cyto}Δ*bisC*), LLS662 (*cpxA**), and LLS690 (*cpxA** Δ*cpxR*), we grew cultures aerobically overnight in LB at 37°C. We prepared the samples for immunoblot analysis after 16 h of growth.

To investigate whether CpxRA activation due to NlpE overproduction induces MsrP production, we grew WT and CA612 (Δ*metA* Δ*3msr*^{cyto}Δ*bisC*) cells harboring empty vector or pNlpE aerobically in LB supplemented with ampicillin at 37°C until an OD_{600} of 0.5 was reached. We then added 0.1 mM IPTG and, after 2 h, prepared the samples for immunoblot analysis.

For immunoblot analysis of MsrP production in each sample, equivalent cell densities (normalized by A_{600}) were pelleted by centrifugation (3,000 g, 5 min). Each sample was suspended in Laemmli SDS sample buffer and heated for 10 min at 95 °C. We resolved the samples on a 12% Tris-glycine SDS-PAGE gel. For immunoblot analysis, we transferred the resolved proteins to 0.2-μm nitrocellulose membranes, which we then probed with anti-MsrP antibody (provided by the Jean-François Collet Lab, de Duve Institute, UCLouvain), followed by an HRP-conjugated anti-guinea pig IgG secondary antibody (Sigma-Aldrich). We

imaged the chemiluminescence signals using an ImageQuant Las4000 camera (GE Healthcare). The presented results are representative of at least three independent experiments.

In Vivo Analysis of Lpp Impairment after *N*-ChT Exposure by Gel Shift Assays. WT cells grew aerobically in LB at 37 °C for approximately 2 h (corresponding to approximately four cell-doubling cycles) until an OD_{600} of 0.5 was reached. At this point, we split the cultures into five tubes and added different concentrations of *N*-ChT (0, 0.5, 1, 1.5, and 2 mM). Before the addition of *N*-ChT (t = 0) and at different time points (30 min, 1 h, 1.5 h, 2 h, 3 h), equivalent cell densities (normalized by A_{600}) were pelleted by centrifugation (3,000 g, 5 min).

To compare the impact of *N*-ChT with the impact of copper on Lpp, we added 2 mM *N*-ChT and 3 mM $CuSO_4$ to a WT culture with an OD_{600} of 0.5, and equivalent cell densities (normalized by A_{600}) were pelleted by centrifugation 1 h after the addition of stress.

Each sample was suspended in Laemmli SDS sample buffer and heated for 10 min at 95 °C. We resolved the samples on a 16% tricine SDS-PAGE gel (49) at 125 V for 2.5 h. For immunoblot analysis, we transferred the resolved proteins to 0.2-µm nitrocellulose membranes, which we then probed with anti-Lpp antibody (provided by the Jean-François Collet Lab, de Duve Institute, UCLouvain), followed by an HRP-conjugated anti-rabbit IgG secondary antibody (Promega). We imaged chemiluminescence signals using an ImageQuant Las4000 camera (GE Healthcare).

Data, Materials, and Software Availability. All study data are included in the article and/or *SI Appendix*.

ACKNOWLEDGMENTS. We thank the members of the Ezraty and Py groups for comments on the manuscript, advice, and discussions. We thank Eric Cascales (Laboratoire d'Ingénierie des Systèmes Macromoléculaires), Romé Voulhoux (Laboratoire de Chimie Bactérienne), and Pauline Leverrier (de Duve Institute, UCLouvain) for providing antibodies. This work was supported by grants from the Agence Nationale Recherche (#ANR-21-CE15-0039 NeutrOX) and the Centre National de la Recherche Scientifique (CNRS) (#PICS-PROTOX). C.A. was supported by the Fondation pour la Recherche Médicale, (#FDT202106012778).

1. J. E. Galán, Salmonella Typhimurium and inflammation: A pathogen-centric affair. *Nat. Rev Microbiol.* **19**, 716–725 (2021).
2. C. C. Winterbourn, A. J. Kettle, Redox reactions and microbial killing in the neutrophil phagosome. *Antioxid Redox. Signal* **18**, 642–660 (2013).
3. S. J. Klebanoff, A. J. Kettle, H. Rosen, C. C. Winterbourn, W. M. Nauseef, Myeloperoxidase: A front-line defender against phagocytosed microorganisms. *J. Leukoc. Biol.* **93**, 185–198 (2013).
4. N. Schürmann *et al.*, Myeloperoxidase targets oxidative host attacks to Salmonella and prevents collateral tissue damage. *Nat. Microbiol.* **2**, 16268 (2017).
5. M. Rhen, Salmonella and reactive oxygen species: A love-hate relationship. *J. Innate. Immun.* **11**, 216–226 (2019).
6. W. S. da Cruz Nizer, V. Inkovskiy, J. Overhage, Surviving reactive chlorine stress: Responses of gram-negative bacteria to hypochlorous acid. *Microorganisms* **8**, 1220 (2020).
7. B. Ezraty, A. Gennaris, F. Barras, J.-F. Collet, Oxidative stress, protein damage and repair in bacteria. *Nat. Rev. Microbiol.* **15**, 385–396 (2017).
8. W. Vogt, Oxidation of methionyl residues in proteins: Tools, targets, and reversal. *Free Radic. Biol. Med.* **18**, 93–105 (1995).
9. N. Brot, H. Weissbach, Peptide methionine sulfoxide reductase: Biochemistry and physiological role. *Biopolymers* **55**, 288–296 (2000).
10. R. Grimaud *et al.*, Repair of oxidized proteins: Identification of a new methionine sulfoxide reductase. *J. Biol. Chem.* **276**, 48915–48920 (2001).
11. Z. Lin *et al.*, Free methionine-(R)-sulfoxide reductase from Escherichia coli reveals a new GAF domain function. *Proc. Natl. Acad. Sci. U.S.A.* **104**, 9597–602 (2007).
12. S. Boschi-Muller, A. Olry, M. Antoine, G. Branlant, The enzymology and biochemistry of methionine sulfoxide reductases. *Biochim. Biophys. Acta (BBA) - Proteins Proteomics*, **1703** 231–238 (2005).
13. B. Kauffmann, A. Aubry, F. Favier, The three-dimensional structures of peptide methionine sulfoxide reductases: Current knowledge and open questions. *Biochim. Biophys. Acta (BBA) - Proteins Proteomics* **1703**, 249–260 (2005).
14. N. Brot, L. Weissbach, J. Werth, H. Weissbach, Enzymatic reduction of protein-bound methionine sulfoxide. *Proc. Natl. Acad. Sci. U.S.A.* **78**, 2155–2158 (1981).
15. B. Ezraty, J. Bos, F. Barras, L. Aussel, Methionine sulfoxide reduction and assimilation in Escherichia coli: New role for the biotin sulfoxide reductase BisC. *J. Bacteriol.* **187**, 231–237 (2005).
16. L. A. Denkel *et al.*, Methionine sulfoxide reductases are essential for virulence of Salmonella Typhimurium. *PLoS One* **6**, e26974 (2011).
17. R. Sarkhel, Methionine sulfoxide reductase A of Salmonella Typhimurium interacts with several proteins and abets in its colonization in the chicken. *Biochim. Biophys. Acta (BBA) - General Subjects*, 3238–3245 (2017).
18. A. Gennaris *et al.*, Repairing oxidized proteins in the bacterial envelope using respiratory chain electrons. *Nature* **528**, 409–412 (2015).
19. C. Andrieu, A. Vergnes, L. Loiseau, L. Aussel, B. Ezraty, Characterisation of the periplasmic methionine sulfoxide reductase (MsrP) from Salmonella Typhimurium. *Free Radic. Biol. Med.* **160**, 506–512 (2020).
20. A. Hitchcock *et al.*, Roles of the twin-arginine translocase and associated chaperones in the biogenesis of the electron transport chains of the human pathogen Campylobacter jejuni. *Microbiol. (N Y)* **156**, 2994–3010 (2010).
21. W. Gottardi, M. Nagl, N-chlorotaurine, a natural antiseptic with outstanding tolerability. *J. Antimicrobial. Chemother.* **65**, 399–409 (2010).
22. M. Nagl, M. W. Hess, K. Pfaller, P. Hengster, W. Gottardi, Bactericidal activity of micromolar N-Chlorotaurine: Evidence for its antimicrobial function in the human defense system. *Antimicrob. Agents Chemother.* **44**, 2507–2513 (2000).
23. T. L. Raivio, Envelope stress responses and Gram-negative bacterial pathogenesis. *Mol. Microbiol.* **56**, 1119–1128 (2005).
24. X. Liang *et al.*, Characterization of methionine oxidation and methionine sulfoxide reduction using methionine-rich cysteine-free proteins. *BMC Biochem.* **13**, 1–10 (2012).
25. S. el Hajj *et al.*, HprSR is a reactive chlorine species-sensing, two-component system in Escherichia coli. *J. Bacteriol.* **204**, e0044921 (2022).
26. A. Delhaye, G. Laloux, J.-F. Collet, The lipoprotein Nlpe is a Cpx sensor that serves as a sentinel for protein sorting and folding defects in the Escherichia coli envelope. *J. Bacteriol.* **201**, e00611-18 (2019).
27. S. Subramaniam *et al.*, Contribution of the Cpx envelope stress system to metabolism and virulence regulation in Salmonella enterica serovar Typhimurium. *PLoS One* **14**, e0211584 (2019).
28. A. Pezza, L. B. Pontel, C. López, F. C. Soncini, Compartment and signal-specific codependence in the transcriptional control of Salmonella periplasmic copper homeostasis. *Proc. Natl. Acad. Sci. U.S.A.* **113**, 11573–11578 (2016).
29. K. Yamamoto, A. Ishihama, Characterization of copper-inducible promoters regulated by CpxA/CpxR in Escherichia coli. *Biosci. Biotechnol. Biochem.* **70**, 1688–1695 (2006).
30. C. J. Kershaw, The expression profile of Escherichia coli K-12 in response to minimal, optimal and excess copper concentrations. *Microbiology (N Y)* **151**, 1187–1198 (2005).
31. K. L. May, K. M. Lehman, A. M. Mitchell, M. Grabowicz, A stress response monitoring lipoprotein trafficking to the outer membrane. *mBio* **10** (2019).
32. Y. Hirano, Md. M. Hossain, K. Takeda, H. Tokuda, K. Miki, Structural studies of the Cpx pathway activator NlpE on the outer membrane of Escherichia coli. *Structure* **15**, 963–976 (2007).
33. C. López, S. K. Checa, F. C. Soncini, CpxR/CpxA controls *scsABCD* transcription to counteract copper and oxidative stress in Salmonella enterica Serovar Typhimurium. *J. Bacteriol.* **200**, e00126-18 (2018).
34. P. N. Danese, T. J. Silhavy, CpxP, a stress-combative member of the Cpx regulon. *J. Bacteriol.* **180**, 831–839 (1998).
35. L. A. Denkel, M. Rhen, F.-C. Bange, Biotin sulfoxide reductase contributes to oxidative stress tolerance and virulence in Salmonella enterica serovar Typhimurium. *Microbiology (Reading)* **159**, 1447–1458 (2013).
36. S. Hunke, J.-M. Betton, Temperature effect on inclusion body formation and stress response in the periplasm of Escherichia coli. *Mol. Microbiol.* **50**, 1579–1589 (2003).
37. R. G. Midwinter, F. C. Cheah, J. Moskovitz, M. C. Vissers, C. C. Winterbourn, IκB is a sensitive target for oxidation by cell-permeable chloramines: Inhibition of NF-κB activity by glycine chloramine through methionine oxidation. *Biochem. J.* **396**, 71–78 (2006).
38. M. B. Grisham, M. M. Jefferson, D. F. Melton, E. L. Thomas, Chlorination of endogenous amines by isolated neutrophils. Ammonia-dependent bactericidal, cytotoxic, and cytolytic activities of the chloramines. *J. Biol. Chem.* **259**, 10404–10413 (1984).
39. S. Bury-Moné *et al.*, Global analysis of extracytoplasmic stress signaling in Escherichia coli. *PLoS Genet.* **5**, e1000651 (2009).
40. S. D. Gupta, H. C. Wu, P. D. Rick, A Salmonella Typhimurium genetic locus which confers copper tolerance on copper-sensitive mutants of Escherichia coli. *J. Bacteriol.* **179**, 4977–4984 (1997).
41. S. Nakayama, H. Watanabe, Involvement of cpxA, a sensor of a two-component regulatory system, in the pH-dependent regulation of expression of Shigella sonnei virF gene. *J. Bacteriol.* **177**, 5062–5069 (1995).
42. G. Jubelin *et al.*, CpxR/OmpR Interplay Regulates Curli Gene Expression in Response to Osmolarity in *Escherichia coli*. *J. Bacteriol.* **187**, 2038–2049 (2005).
43. G. J. Leclerc, C. Tartera, E. S. Metcalf, Environmental regulation of Salmonella typhi invasion-defective mutants. *Infect. Immun.* **66**, 682–691 (1998).
44. H. Huang *et al.*, Regulation of the two-component regulator CpxR on aminoglycosides and β-lactams resistance in Salmonella enterica serovar Typhimurium. *Front. Microbiol.* **7**, 604 (2016).
45. W. Jing, J. Liu, S. Wu, X. Li, Y. Liu, Role of cpxA mutations in the resistance to aminoglycosides and β-Lactams in Salmonella enterica serovar Typhimurium. *Front. Microbiol.* **12**, 604079 (2021).
46. I. Jo *et al.*, Structural basis for HOCl recognition and regulation mechanisms of HypT, a hypochlorite-specific transcriptional regulator. *Proc. Natl. Acad. Sci. U.S.A.* **116**, 3740–3745 (2019).
47. K. A. Datsenko, B. L. Wanner, One-step inactivation of chromosomal genes in Escherichia coli K-12 using PCR products. *Proc. Natl. Acad. Sci. U.S.A.* **97**, 6640–6645 (2000).
48. S. A. Haney *et al.*, Increased retention of functional fusions to toxic genes in new two-hybrid libraries of the E. coli strain MG1655 and B. subtilis strain 168 genomes, prepared without passaging through E. coli. *BMC Genom.* **4**, 36 (2003).
49. H. Schägger, Tricine–SDS-PAGE. *Nat. Protoc.* **1**, 16–22 (2006).